university of groningen

University Medical Center Groningen

University of Groningen

Improving the time control of the Subboreal/Subatlantic transition in a Czech peat sequence by 14C wiggle-matching

Speranza, A.; Plicht, J. van der; Geel, B. van

Published in:
Quaternary Science Reviews

DOI:
10.1016/S0277-3791(99)00108-0

IMPORTANT NOTE: You are advised to consult the publisher's version (publisher's PDF) if you wish to cite from it. Please check the document version below.

Document Version
Publisher's PDF, also known as Version of record

Publication date:
2000

Link to publication in University of Groningen/UMCG research database

Citation for published version (APA):
Speranza, A., Plicht, J. V. D., & Geel, B. V. (2000). Improving the time control of the Subboreal/Subatlantic transition in a Czech peat sequence by 14C wiggle-matching. *Quaternary Science Reviews*, *19*(16), 1589-1604. https://doi.org/10.1016/S0277-3791(99)00108-0

Copyright
Other than for strictly personal use, it is not permitted to download or to forward/distribute the text or part of it without the consent of the author(s) and/or copyright holder(s), unless the work is under an open content license (like Creative Commons).

The publication may also be distributed here under the terms of Article 25fa of the Dutch Copyright Act, indicated by the “Taverne” license. More information can be found on the University of Groningen website: https://www.rug.nl/library/open-access/self-archiving-pure/taverne-amendment.

Take-down policy
If you believe that this document breaches copyright please contact us providing details, and we will remove access to the work immediately and investigate your claim.

Downloaded from the University of Groningen/UMCG research database (Pure): http://www.rug.nl/research/portal. For technical reasons the number of authors shown on this cover page is limited to 10 maximum.

PERGAMON

Quaternary Science Reviews 19 (2000) 1589–1604

QSR

Improving the time control of the Subboreal/Subatlantic transition in a Czech peat sequence by ^{14}C wiggle-matching

A. Speranza[a,*], J. van der Plicht[b], B. van Geel[a]

[a]*Hugo de Vries Laboratory, University of Amsterdam, Kruislaan 318, NL-1098 SM Amsterdam (The Netherlands Centre for Geo-ecological Research, ICG), Netherlands*

[b]*Centre for Isotope Research, University of Groningen, Nijenborgh 4, NL-9747 AG Groningen (The Netherlands Centre for Geo-ecological Research, ICG), Netherlands*

Abstract

To achieve an optimal time-control for a late Subboreal to early Subatlantic peat sequence from Pančavská Louka in the Czech Republic, different strategies are applied to convert a series of radiocarbon dates into a calendar time-scale. The methods of selection and preparation of the samples for AMS ^{14}C dating are presented. The results of calibrating single radiocarbon dates are compared with a ^{14}C wiggle-match strategy. As the accumulation rate of the peat was not constant, the concentrations of arboreal pollen are used to estimate the accumulation rate changes and to correct for these changes. The resulting time-control represents the best solution for this peat sequence with the methods currently available. © 2000 Elsevier Science Ltd. All rights reserved.

1. Introduction

The conversion of radiocarbon dates into calendar ages is complicated by the nonlinearity of the calibration curve, i.e. the presence of wiggles due to past variations in the atmospheric ^{14}C content (de Vries, 1958; Suess, 1970; Stuiver et al., 1998). In particular, the calibration of radiocarbon dates at approximately 2500–2450 BP is problematic due to a "plateau" (known as the "Hallstatt-plateau") in the calibration curve (Kilian et al., 1995, 2000) (Fig. 1a and Fig. 2). A decrease in solar activity caused an increase in production of ^{14}C, and thus a sharp rise in $\Delta^{14}C$, beginning at approximately 850 cal (calendar years) BC (Fig. 1b). Between approximately 760 and 420 cal BC (corresponding to 2500–2425 BP), the concentration of ^{14}C returned to "normal" values. These events are mirrored in the calibration curve as a sharp descent between 850 and 760 cal BC (2700–2450 BP) — corresponding to the increase in $\Delta^{14}C$ — and a plateau between 760 and 420 cal BC (2500–2425 BP) — corresponding to the decrease of the excess in ^{14}C (Fig. 1). A consequence of the decreasing atmospheric ^{14}C concentration between 760 and 420 cal BC is that plants and animals that died during that time interval now display similar radiocarbon ages, scattering around 2450 BP. The calibration of these radiocarbon ages into calendar ages gives a probability range covering approximately 340 calendar years, from 760 to 420 cal BC (Fig. 2). This lack of accuracy for calibrated results is problematic in palaeobotanical and archaeological reconstructions if no other absolute dating method providing a calendar time-scale (i.e. dendrochronology, varved sequences) can be additionally applied. A solution is given by the wiggle-match strategy (van Geel and Mook, 1989), where a stratigraphic sequence of ^{14}C dates is matched to the wiggles of the calibration curve. This is analogous to wiggle-matching of floating tree rings to the calibration curve (Pearson, 1986). The application of the wiggle-match dating strategy (WMD) can also provide evidences for a reservoir effect in a sequence, as demonstrated by Kilian et al. (1995) for raised bogs.

An important application of WMD is the research on the apparent existence of a link between the decrease in solar activity at 850 cal BC and the climatic deterioration occurring at the same time (Davis, 1994; Denton and Karlen, 1973; Karlen and Kuylenstierna, 1996; van Geel et al., 1998, 1999; Jirikowic et al., 1993; Magny, 1993, 1999). Evidence for such a link can be the positive correlation between changing solar activity proxies (the cosmogenic isotopes ^{14}C and ^{10}Be) and geological climate proxies. Such a relationship is feasible only when time

* Corresponding author. Tel.: 0031-20-5257666; fax: 0031-20-5257878.

E-mail address: speranza@bio.uva.nl (A. Speranza).

0277-3791/00/$ - see front matter © 2000 Elsevier Science Ltd. All rights reserved.
PII: S0277-3791(99)00108-0

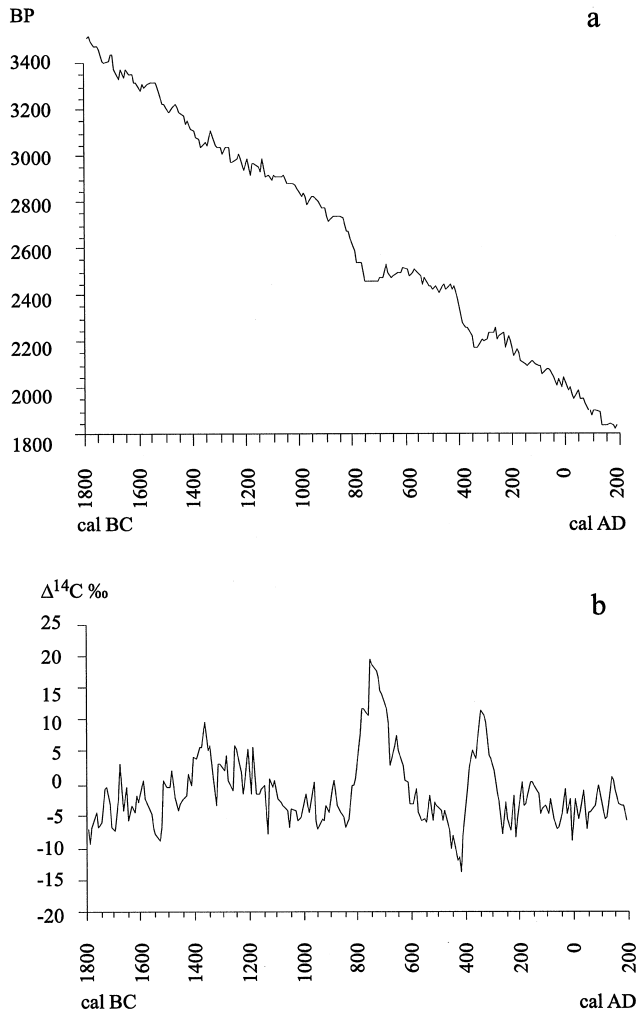

Fig. 1. Radiocarbon calibration curve (a) and $\Delta^{14}C$ detrended for the magnetic field (b) between 1800 cal BC and 200 cal AD. Data from the INTCAL 98 curve (Stuiver et al., 1998).

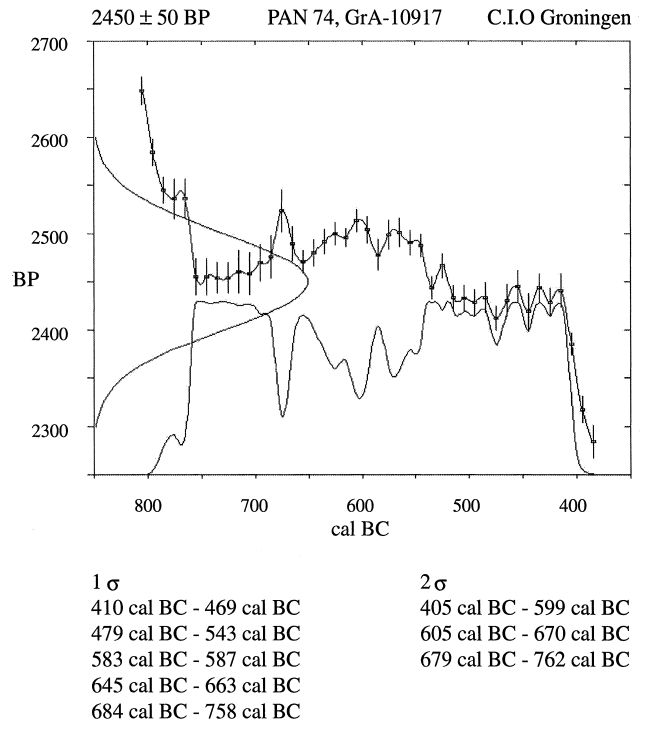

Fig. 2. Example of the calibration of a radiocarbon date (2450 ± 50 BP) around the Hallstatt plateau. The probability distribution in calendar years yields almost four centuries.

control is precise. The application of WMD can provide the required precision, but it requires application in those parts of the calibration curve where pronounced, characteristic wiggles are present because the shape of a single wiggle of the calibration curve has to be recognised in the sediment or peat sequence for the series of ^{14}C dates to be matched. This is usually an expensive strategy, as it requires a great number of radiocarbon dates by AMS of selected material (leaves, seeds and other above-ground material).

Palaeoecological analyses of a sequence from the peat bog of Pančavská Louka (Czech Republic) provided data on climatic change towards cooler, moister conditions at the Subboreal–Subatlantic transition. To reconstruct the phases of this climatic event, an accurate time-control was needed. This could be achieved by using the ^{14}C wiggle-match dating strategy.

2. Materials and methods

2.1. Peat samples collection and preparation

The peat bog of Pančavská Louka (50°45′10″ N, 15°32′50″E) is located at a height of 1320 m in the Krkonoše Mountains (Giant Mountains), in the Czech Republic. It belongs to the complex of montane raised bogs (Neuhäuslova et al., 1998), and at present it is approximately 1 km in diameter (Fig. 3). The sampled peat section represents the period from 5320 ± 60 BP (GrA-6326) to the present time (1996 AD). Here we present the dating procedures and the conversion from a radiocarbon to a calendar time-scale by means of WMD for the period between 3100 and 1900 BP.

Fluctuations in the total arboreal pollen concentration mainly depend on changes in the accumulation rate of the peat in the absence of marked human influence (Middeldorp, 1982). Such fluctuations can be used in the wiggle-matching procedure to model a distance between subsequent ^{14}C samples that takes into account changes in the peat accumulation rate. We also show a relevant selection of pollen and macrofossil data (peat forming plants) for the time range between 3100 and 1900 BP. The complete micro- and macrofossil record will be published in a future paper.

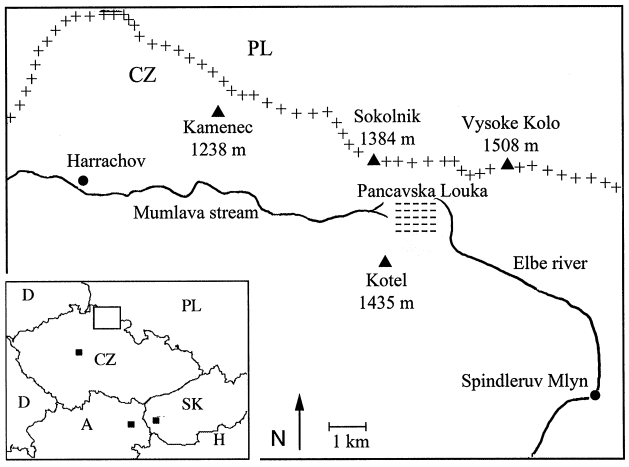

Fig. 3. Map and location of the area.

For the time interval presented, 29 samples were radiocarbon dated by AMS at the Centre for Isotope Research of the University of Groningen. The selection and preparation of the samples for the AMS dating is a complex procedure comprising many steps, from the collection of the peat sequence in the field to the preparation of graphite targets for the AMS. We briefly describe each step below.

2.2. Sampling, preparation and analysis of the macro- and microfossils

The material was collected by digging a pit in the bog, exposing a clean vertical profile and collecting the peat by pressing metal boxes ($50 \times 15 \times 10$ cm; open at one side) into the profile. Full boxes were removed from the profile, covered with plastic film to prevent contamination, brought to the laboratory and preserved at a temperature of 3°C. Before sub-sampling the material in the metal boxes, the outside layer of approximately 2 cm of peat was removed to avoid contamination. Contiguous horizontal slices of 0.5 cm thickness were cut. From these slices, one sample for pollen analysis and one for macrofossil analysis were taken, and the remaining material was preserved. The analysis of micro- and macrofossils was carried out every cm. The radiocarbon samples were selected from the macrofossil samples.

The macrofossil samples (3–8 cc) were boiled in KOH (5%) to dissolve humic and fulvic acids. Subsequently, the material was sieved (100 μm mesh); the material on the sieve was preserved in demineralized water. A few drops of HCl (5%) were added to prevent further decomposition and contamination by bacteria or fungi. Macrofossil analysis was carried out on a binocular microscope (magnification 10× and 20×); the percentage in volume of each peat constituent within the total composition of the sample was visually estimated. The sample was split in subsamples which were observed in water in a Petri dish. The Petri dish was divided in sectors in order to avoid overlapping with already analysed parts of the subsample. A plus (+) in the curve of a taxon indicates that this taxon was present in the sample in such a low quantity that the attribution of a volume percentage was not realistic.

Microfossils samples were treated with KOH and acetolysed according to the method of Faegri and Iversen (1989). The identification of pollen grains was based on Moore et al. (1991). Rare taxa are indicated with a plus (+).

2.3. Preparation of the samples for radiocarbon dating

The selection of macrofossils for radiocarbon dating was undertaken using a binocular microscope (magnifications 10× and 20×). A number of samples showed traces of fossil fungal infection (mycelium). An empirical fungal infection coefficient (FIC) was introduced to tentatively express the degree of fungal contamination of the original sample. A FIC, going from 0 (very low degree of decomposition; no visible infection by fungi) to 5 (very decomposed with many hyphae) was given to each sample. Leaves and branches of *Sphagnum* species (peat moss) were collected for radiocarbon dating. The advantage of mosses for dating is that they represent the vegetation of former surfaces of the bog. On the contrary, Spermatophyta (flowering plants) have roots that penetrate in deeper levels making bulk ^{14}C samples too young. An advantage of *Sphagna* on other mosses, from a dating point of view, is their active acidification of the environment (Clymo, 1963) which inhibits bacteria from decomposing *Sphagnum*.

When a sufficient quantity of *Sphagnum* was collected in a Petri dish, the cleaning phase started: each leaf and branch was cleaned (all material other than *Sphagnum* was removed, i.e. ericaceous roots, fungal mycelium) and moved to another Petri dish in demineralized water. Material infected by fungi or too decomposed material was not used. A threefold repetition of this procedure ensured that the sample was composed of pure *Sphagnum* and that no other macroscopic remains were present. However, even if the selected material that constituted the radiocarbon sample was cleaned from any impurity visible under the binocular microscope, it was still possible that some invisible contaminants were present. The FIC is a tentative measure of this possible contamination. In each step of the preparation of the samples for radiocarbon dating, chemically pure reagents (pA) and demineralized water were used.

Acid–Alkali–Acid treatment: The purpose of this treatment is to further eliminate every eventual remaining trace of humic and fulvic acids and to eliminate the bacterial CO_2 formed during the decomposition processes (Mook and Streurman, 1983).

The selected *Sphagnum* remains were placed in HCl (4%) for approximately 1 h. The material was then sieved and rinsed with demineralized water and subsequently put in KOH 1% warm and then sieved and rinsed again. The HCl (4%) treatment was repeated for 1 h. The material was finally thoroughly rinsed with demineralized water, put in glass bottles and dried in the oven at 80°C for 24 h.

Combustion and CO_2 production: The samples were combusted in an automatic CN Analyser Carlo Erba 1500, coupled to a Micromass Optima IRMS, enabling high-precision $\delta^{13}C$ and $\delta^{15}N$ determinations. The CO_2 produced is trapped cryogenically (Aerts-Bijma et al., 1997).

Graphitization and target production: The CO_2 produced by the CN Analyser is transferred to the graphitization room. For the production of graphite, the method of reduction under an excess of hydrogen gas with iron powder as catalyst is used (Vogel et al., 1984):

$$CO_2 + 2H_2 \rightarrow (Fe) \rightarrow C + 2H_2O.$$

Table 1
List of the AMS ^{14}C dates of the peat sequence of Pančavská Louka for the 110-56 cm depth interval (between 3100 and 1900 BP). The sample code is that used by the Radiocarbon Laboratory of Groningen University (GrA). The samples with a star (*) are composed of *Sphagnum* and seeds of Ericales and of seeds of *Carex*; all the other samples are pure *Sphagnum*. FIC is fungal infection coefficient. Large errors are caused by small sample size

Depth (cm)	Sample code	Radiocarbon age BP	FIC
56.0*	GrA-10910	1940 ± 50	0.5
58.0	GrA-10580	2115 ± 75	1
59.0	GrA-10912	1910 ± 50	0.5
62.0	GrA-7099	2130 ± 60	0
64.0	GrA-10524	2035 ± 60	0
66.0	GrA-10564	2230 ± 55	0
68.0	GrA-10561	2255 ± 55	0
70.0	GrA-7479	2130 ± 60	0
72.0	GrA-10914	2420 ± 50	0.5
73.0	GrA-9824	2515 ± 55	0
74.0	GrA-10917	2450 ± 50	0
75.0	GrA-10523	2330 ± 60	0
77.0	GrA-10089	2480 ± 35	1
79.0	GrA-9823	2455 ± 45	0
81.0	GrA-7481	2540 ± 100	0
83.0	GrA-11999	2470 ± 50	0.5
84.0	GrA-7482	2650 ± 60	0
86.0	GrA-7483	2640 ± 60	0
88.0	GrA-10579	2565 ± 90	0.5
89.0*	GrA-10919	2880 ± 50	1
90.0	GrA-10520	2790 ± 60	1
92.0	GrA-9822	2775 ± 45	0
94.0	GrA-9821	2885 ± 45	0
96.0	GrA-9819	2925 ± 45	0
98.0	GrA-10519	2915 ± 60	0–0.5
100.0	GrA-10518	2900 ± 60	0
102.0	GrA-10560	3135 ± 60	1–1.5
104.0	GrA-10516	2875 ± 60	0.5
110.0	GrA-9818	3145 ± 45	0

An automatic system presses the graphite powder into a target holder that fits in the carousel of the AMS ion source.

AMS dating: The Groningen AMS accelerator is a tandetron operating at 2.5 MV. Performance tests on the $^{13}\delta$ and on the $^{14}C/^{12}C$ ratio showed a precision better than 2‰ and 0.5 pMC, respectively (Mous et al., 1995). ^{14}C dates are corrected for isotopic fractionation to $\delta^{13}C = -25‰$, as measured by the AMS itself.

The results of the AMS ^{14}C dating are shown in Table 1. These dates were both calibrated and wiggle-matched, so that the results of both approaches can be compared and evaluated.

3. Conversion of the radiocarbon time-scale into calendar time-scale

3.1. Calibration

We calibrated the ^{14}C dates with the program Cal25 (van der Plicht, 1993) updated with the new calibration data of Stuiver et al. (1998). The results are shown in Table 2. Calibration of ^{14}C often yields problematic interpretations in palaeoecology or archaeology (Dumayne et al., 1995) because the resulting probability distribution is no longer Gaussian, often with several maxima and minima (van der Plicht and Mook, 1987). Often the results of calibration are sufficient for the aims of the research. The aim of our research however, is to precisely date the climatic change at around 2700 BP and to find periodic cycles in vegetation succession patterns by applying spectral analysis to the palaeobotanical data. In this paper we focus on the time control aspects; spectral analysis will be published in a subsequent paper. Therefore, we need to attribute a single age to each level, i.e. we have to express the result of the calibration in a single value. One can choose either the mid-point between the two dates that enclose the 95.4% confidence interval (Bennett, 1995), or the calendar age corresponding to the intersection of the radiocarbon age without its standard deviation and the calibration curve ("best fit") (Table 3). Both procedures are statistically not completely justifiable and thus errors in the time-control are introduced. Wiggle-matching of the dates is an attractive alternative approach.

3.2. Wiggle-matching

3.2.1. Wiggle-matching with a linear depth scale

Wiggle-match dating (WMD) of a sequence of radiocarbon dates means plotting these dates in their stratigraphical order, so that they are best matched with the calibration curve (van Geel and Mook, 1989). This strategy makes use of the past atmospheric ^{14}C fluctuations (wiggles) as they are observed in the ^{14}C record of

Table 2
Results of the individual calibration of the dates of Pančavská Louka. The dates are calibrated with the Groningen program Cal25, the updating of Cal20 (van der Plicht, 1993) using the INTCAL 98 calibration curve (Stuiver et al., 1998)

Sample and ^{14}C age	1σ	2σ
PAN 56.0	98 cal AD–126 cal AD	192 cal AD–212 cal AD
1940 ± 50 BP	22 cal AD–90 cal AD	148 cal AD–176 cal AD
GrA-10910	4 cal AD–11 cal AD	45 cal BC–135 cal AD
PAN 58.0	7 cal BC–3 cal BC	43 cal AD–48 cal AD
2115 ± 75 BP	205 cal BC–43 cal BC	262 cal BC–25 cal AD
GrA-10580	228 cal BC–222 cal BC	361 cal BC–271 cal BC
	348 cal BC–320 cal BC	
PAN 59.0	198 cal AD–207 cal AD	2 cal AD–232 cal AD
1910 ± 50 BP	163 cal AD–168 cal AD	17 cal BC–14 cal BC
GrA-10912	49 cal AD–133 cal AD	
	26 cal AD–42 cal AD	
PAN 62.0	79 cal BC–54 cal BC	11 cal BC–0 cal AD
2130 ± 60 BP	204 cal BC–88 cal BC	31 cal BC–21 cal BC
GrA-7099	227 cal BC–223 cal BC	260 cal BC–39 cal BC
	347 cal BC–321 cal BC	359 cal BC–272 cal BC
PAN 64.0	41 cal AD–50 cal AD	108 cal AD–110 cal AD
2035 ± 60 BP	113 cal BC–27 cal AD	178 cal BC–81 cal AD
GrA-10524		200 cal BC–187 cal BC
PAN 66.0	221 cal BC–205 cal BC	396 cal BC–173 cal BC
2230 ± 55 BP	265 cal BC–229 cal BC	
GrA-10564	319 cal BC–266 cal BC	
	379 cal BC–350 cal BC	
PAN 68.0	219 cal BC–208 cal BC	186 cal BC–180 cal BC
2255 ± 55 BP	296 cal BC–231 cal BC	400 cal BC–200 cal BC
GrA-10561	315 cal BC–310 cal BC	
	390 cal BC–352 cal BC	
PAN 70.0	79 cal BC–54 cal BC	11 cal BC–0 cal AD
2130 ± 60 BP	204 cal BC–88 cal BC	31 cal BC–21 cal BC
GrA-7479	227 cal BC–223 cal BC	260 cal BC–39 cal BC
	347 cal BC–321 cal BC	359 cal BC–272 cal BC
PAN 72.0	522 cal BC–404 cal BC	566 cal BC–399 cal BC
2420 ± 50 BP	540 cal BC–528 cal BC	594 cal BC–573 cal BC
GrA-10914	714 cal BC–702 cal BC	668 cal BC–612 cal BC
	756 cal BC–716 cal BC	761 cal BC–680 cal BC
PAN 73.0	527 cal BC–524 cal BC	424 cal BC–412 cal BC
2515 ± 55 BP	700 cal BC–540 cal BC	441 cal BC–426 cal BC
GrA-9824	792 cal BC–756 cal BC	465 cal BC–450 cal BC
		494 cal BC–483 cal BC
		510 cal BC–497 cal BC
		798 cal BC–513 cal BC
PAN 74.0	469 cal BC–410 cal BC	599 cal BC–405 cal BC
2450 ± 50 BP	543 cal BC–479 cal BC	670 cal BC–605 cal BC
GrA-10917	587 cal BC–583 cal BC	762 cal BC–679 cal BC
	663 cal BC–645 cal BC	
	758 cal BC–684 cal BC	
PAN 75.0	216 cal BC–211 cal BC	224 cal BC–204 cal BC
2330 ± 60 BP	246 cal BC–233 cal BC	323 cal BC–226 cal BC

Table 2. Continued

GrA-10523	289 cal BC–257 cal BC	543 cal BC–346 cal BC
	413 cal BC–355 cal BC	661 cal BC–649 cal BC
	429 cal BC–421 cal BC	758 cal BC–685 cal BC
	451 cal BC–439 cal BC	
	486 cal BC–464 cal BC	
	515 cal BC–488 cal BC	
PAN 77.0	530 cal BC–520 cal BC	442 cal BC–411 cal BC
2480 ± 35 BP	596 cal BC–538 cal BC	466 cal BC–449 cal BC
GrA-10089	669 cal BC–609 cal BC	765 cal BC–482 cal BC
	727 cal BC–680 cal BC	
	747 cal BC–733 cal BC	
	761 cal BC–754 cal BC	
PAN 79.0	442 cal BC–411 cal BC	599 cal BC–407 cal BC
2455 ± 45 BP	467 cal BC–449 cal BC	670 cal BC–607 cal BC
GrA-9823	544 cal BC–482 cal BC	762 cal BC–679 cal BC
	589 cal BC–581 cal BC	
	664 cal BC–642 cal BC	
	759 cal BC–683 cal BC	
PAN 81.0	530 cal BC–520 cal BC	835 cal BC–400 cal BC
2540 ± 100 BP	750 cal BC–535 cal BC	890 cal BC–885 cal BC
GrA-7481	800 cal BC–755 cal BC	
PAN 83.0	420 cal BC–414 cal BC	473 cal BC–409 cal BC
2470 ± 50 BP	438 cal BC–430 cal BC	764 cal BC–476 cal BC
GrA-11999	462 cal BC–453 cal BC	
	567 cal BC–517 cal BC	
	594 cal BC–573 cal BC	
	668 cal BC–611 cal BC	
	761 cal BC–680 cal BC	
PAN 84.0	841 cal BC–790 cal BC	577 cal BC–561 cal BC
2650 ± 60 BP	863 cal BC–850 cal BC	615 cal BC–593 cal BC
GrA-7482	896 cal BC–876 cal BC	631 cal BC–619 cal BC
		681 cal BC–666 cal BC
		928 cal BC–760 cal BC
		970 cal BC–959 cal BC
PAN 86.0	772 cal BC–767 cal BC	579 cal BC–546 cal BC
2640 ± 60 BP	840 cal BC–783 cal BC	637 cal BC–591 cal BC
GrA-7483	861 cal BC–852 cal BC	682 cal BC–665 cal BC
	896 cal BC–876 cal BC	921 cal BC–759 cal BC
		967 cal BC–963 cal BC
PAN 88.0	529 cal BC–522 cal BC	836 cal BC–407 cal BC
2565 ± 90 BP	704 cal BC–539 cal BC	893 cal BC–879 cal BC
GrA-10579	718 cal BC–710 cal BC	
	824 cal BC–756 cal BC	
PAN 89.0	953 cal BC–947 cal BC	1132 cal BC–920 cal BC
2880 ± 50 BP	985 cal BC–976 cal BC	1170 cal BC–1139 cal BC
GrA-10919	1128 cal BC–998 cal BC	1193 cal BC–1173 cal BC
	1187 cal BC–1182 cal BC	1213 cal BC–1199 cal BC
		1255 cal BC–1243 cal BC
PAN 90.0	854 cal BC–840 cal BC	1053 cal BC–824 cal BC
2790 ± 60 BP	877 cal BC–859 cal BC	1087 cal BC–1060 cal BC
GrA-10520	1001 cal BC–895 cal BC	1112 cal BC–1097 cal BC
		1125 cal BC–1117 cal BC
PAN 92.0	879 cal BC–837 cal BC	1006 cal BC–828 cal BC
2775 ± 45 BP	941 cal BC–894 cal BC	
GrA-9822	973 cal BC–957 cal BC	

Table 2. Continued

Sample and ^{14}C age	1σ	2σ
PAN 94.0	1128 cal BC–1000 cal BC	960 cal BC–925 cal BC
2885 ± 45 BP	1187 cal BC–1181 cal BC	1132 cal BC–969 cal BC
GrA-9821		1168 cal BC–1140 cal BC
		1192 cal BC–1174 cal BC
		1212 cal BC–1199 cal BC
		1255 cal BC–1245 cal BC
PAN 96.0	1132 cal BC–1045 cal BC	981 cal BC–980 cal BC
2925 ± 45 BP	1167 cal BC–1140 cal BC	1261 cal BC–999 cal BC
GrA-9819	1192 cal BC–1175 cal BC	1288 cal BC–1282 cal BC
	1212 cal BC–1200 cal BC	
	1254 cal BC–1247 cal BC	
PAN 98.0	1131 cal BC–1006 cal BC	961 cal BC–924 cal BC
2915 ± 60 BP	1166 cal BC–1140 cal BC	1264 cal BC–969 cal BC
GrA-10519	1191 cal BC–1176 cal BC	1294 cal BC–1276 cal BC
	1212 cal BC–1200 cal BC	
	1253 cal BC–1248 cal BC	
PAN 100.0	1131 cal BC–1000 cal BC	963 cal BC–920 cal BC
2900 ± 60 BP	1165 cal BC–1141 cal BC	1261 cal BC–966 cal BC
GrA-10518	1191 cal BC–1176 cal BC	1287 cal BC–1283 cal BC
	1211 cal BC–1201 cal BC	
PAN 102.0	1339 cal BC–1317 cal BC	1283 cal BC–1261 cal BC
3135 ± 60 BP	1357 cal BC–1351 cal BC	1521 cal BC–1286 cal BC
GrA-10560	1458 cal BC–1372 cal BC	
	1494 cal BC–1476 cal BC	
PAN 104.0	956 cal BC–941 cal BC	1135 cal BC–901 cal BC
2875 ± 60 BP	1128 cal BC–973 cal BC	1215 cal BC–1136 cal BC
GrA-10516	1187 cal BC–1181 cal BC	1258 cal BC–1236 cal BC
PAN 110.0	1333 cal BC–1322 cal BC	1342 cal BC–1316 cal BC
3145 ± 45 BP	1453 cal BC–1387 cal BC	1360 cal BC–1348 cal BC
GrA-9818	1492 cal BC–1479 cal BC	1518 cal BC–1370 cal BC

Table 3
Choice of a single calendar age for the radiocarbon dates. The average (middle point) of the probability interval and the calendar age corresponding to the best intersection of the radiocarbon age without standard deviation and the calibration curve are presented

Depth (cm)	Radiocarbon age BP	Middle point of 2σ range	Best fit intersection cal curve
56	1940 ± 50	83 cal AD	71 cal AD
58	2115 ± 75	156 cal BC	121 cal BC
59	1910 ± 50	107 cal BC	82 cal AD
62	2130 ± 60	179 cal BC	171 cal BC
64	2035 ± 60	45 cal BC	43 cal BC
66	2230 ± 55	284 cal BC	287 cal BC
68	2255 ± 55	290 cal BC	375 cal BC
70	2130 ± 60	179 cal BC	171 cal BC
72	2420 ± 50	580 cal BC	446 cal BC
73	2515 ± 55	605 cal BC	679 cal BC
74	2450 ± 50	583 cal BC	532 cal BC
75	2330 ± 60	481 cal BC	397 cal BC
77	2480 ± 35	588 cal BC	587 cal BC
79	2455 ± 45	584 cal BC	737 cal BC
81	2540 ± 100	645 cal BC	782 cal BC
83	2470 ± 50	586 cal BC	684 cal BC
84	2650 ± 60	765 cal BC	805 cal BC
86	2640 ± 60	756 cal BC	803 cal BC
88	2565 ± 90	650 cal BC	791 cal BC
89	2880 ± 50	1087 cal BC	1032 cal BC
90	2790 ± 60	974 cal BC	963 cal BC
92	2775 ± 45	917 cal BC	916 cal BC
94	2885 ± 45	1227 cal BC	1046 cal BC
96	2925 ± 45	1134 cal BC	1183 cal BC
98	2915 ± 60	1109 cal BC	1093 cal BC
100	2900 ± 60	1103 cal BC	1107 cal BC
102	3135 ± 60	1391 cal BC	1410 cal BC
104	2875 ± 60	1079 cal BC	1018 cal BC
110	3145 ± 45	917 cal BC	1412 cal BC

dendrochronologically dated tree rings. These wiggles must be visible in sediment samples as well when plotting ^{14}C dates as a function of depth. By considering the presence of the wiggles in the calibration curve and using their peculiar shape to fit the series of ^{14}C dates from a peat sequence to the calibration curve, the wiggle-match strategy uses the past ^{14}C fluctuations for improving the precision of conversion from radiocarbon to calendar time-scale. In other words, the stratigraphical order of the ^{14}C dates is used to narrow the probability range in calendar ages.

The radiocarbon dates (Table 1) were matched to the recommended decadal calibration curve INTCAL 98 (Stuiver et al., 1998) by the Groningen computer program Cal25, the updating of Cal20 (van der Plicht, 1993). The wiggle-match option of the program allows shifting the data-set vertically and horizontally (in relation to the calibration curve), and to linearly compress or expand it. The horizontal shift option is mainly used for the matching of ^{14}C dates of floating tree ring sequences. The vertical shift option can be used for compensating for the possible existence of a reservoir effect (Kilian et al., 1995), when the sequence of dates do reproduce the wiggle but show older radiocarbon ages. The compression/expansion option simulates a lower, respectively higher peat accumulation rate. This option uses the complete data-set and thus an over-all linear change in the depth scale is assumed. A first, tentative wiggle-match was pursued by matching the complete data-set to the calibration curve (Fig. 4; Table 4).

It is not to be expected that peat deposits have a constant accumulation rate over short spans of time (Kilian et al., 2000). The arboreal pollen concentration curve is mainly influenced by changes in the peat accumulation rate. According to Middeldorp (1982), the pollen deposition rate per year, or pollen influx, is constant for regional arboreal components in raised bog deposits, in absence of marked human impact. High arboreal pollen concentrations indicate that the accumulation rate is low, and low arboreal pollen concentrations point to a high peat accumulation rate.

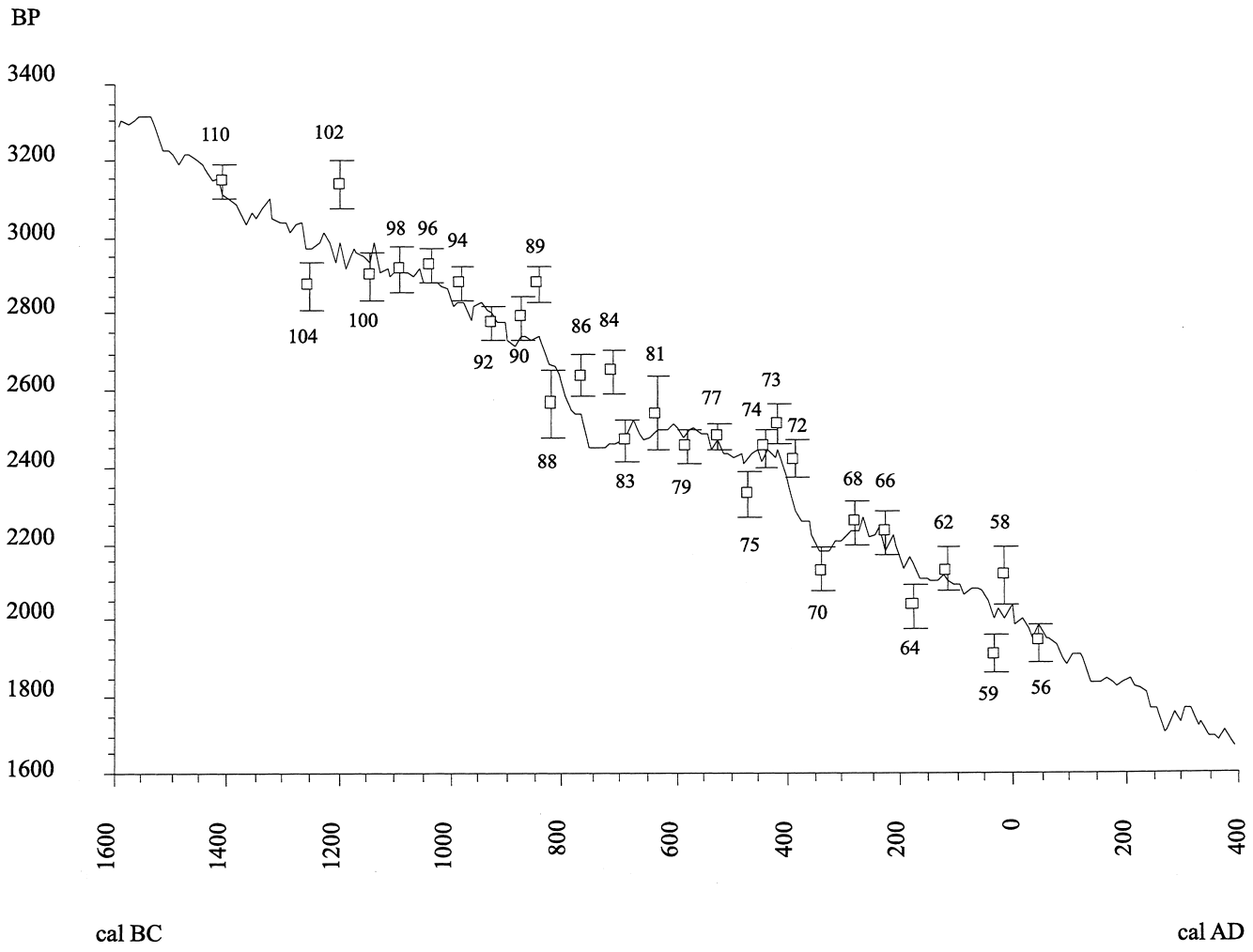

Fig. 4. Wiggle-match of the total set of 29 dates from Pančavská Louka to the INTCAL 98 calibration curve. Each date is given with its standard deviation (error bar) and with its depth in the peat sequence (in cm).

The arboreal pollen concentration curve (Fig. 5) shows that the accumulation rate is not constant. Factors influencing the peat accumulation rate are organic production by the peat-forming vegetation, peat decomposition, and peat compaction rate. Influenced by temperature, precipitation/humidity and trophic conditions, the species composition of peat forming vegetation is the main factor influencing the peat accumulation rate. From the significant changes in peat forming vegetation distinguished in the macrofossil diagram (Fig. 5), we may expect changes in peat accumulation rate. Therefore, the results of this first wiggle-match (Fig. 4) are not accurate enough for our purpose because changes in the peat accumulation rate are not taken into account.

To solve this problem, the data set was divided in sub-datasets, each of which was individually wiggle-matched. The division in sub-datasets was based on the changes in concentration of arboreal pollen (Fig. 5). To reduce noise and short-term changes, we smoothed the concentrations with a low-pass filter. A moving average on each three consecutive samples with weights of 0.25, 0.50 and 0.25 was applied. Based on this smoothed concentration of arboreal pollen, five intervals characterised by having a relatively uniform peat accumulation rate could be distinguished: 110-98, 96-92, 90-86, 84-70 and 68-56 cm, respectively. The results are shown in Fig. 6 and Table 4. In our opinion these results do not yet represent the optimal solution of the dating problem. In the case of the Pančavská Louka sequence, the constantly changing arboreal pollen concentrations (reflecting changing peat accumulation rates) make it rather difficult to choose at which levels to split the dataset to create sub-datasets for WMD. A uniform accumulation rate within each sub-dataset cannot be expected.

3.2.2. Wiggle-matching with inter-sample distance modelled on arboreal pollen concentration

A way to effectively solve the problem of changing peat accumulation rates as reflected in the arboreal pollen (AP) concentration changes is to include these changes in

Table 4
Calendar ages after wiggle-match dating of the complete data set and of the sub-datasets: group 1 (110 to 98 cm); group 2 (96 to 92 cm); group 3 (90 to 86 cm); group 4 (84 to 70 cm); group 5 (68 to 56 cm)

Sub-datasets	Depth (cm)	Radiocarbon Age BP	WMD results Complete dataset	WMD results Sub-datasets
5	56	1940 ± 50	44 cal AD	70 AD
	58	2115 ± 75	16 cal BC	13 AD
	59	1910 ± 50	35 cal BC	14 BC
	62	2130 ± 60	116 cal BC	98 BC
	64	2035 ± 60	175 cal BC	154 BC
	66	2230 ± 55	225 cal BC	210 BC
	68	2255 ± 55	276 cal BC	267 BC
4	70	2130 ± 60	336 cal BC	338 BC
	72	2420 ± 50	389 cal BC	403 BC
	73	2515 ± 55	416 cal BC	435 BC
	74	2450 ± 50	443 cal BC	468 BC
	75	2330 ± 60	470 cal BC	500 BC
	77	2480 ± 35	524 cal BC	565 BC
	79	2455 ± 45	578 cal BC	630 BC
	81	2540 ± 100	631 cal BC	695 BC
	83	2470 ± 50	685 cal BC	760 BC
	84	2650 ± 60	712 cal BC	792 BC
3	86	2640 ± 60	766 cal BC	802 BC
	88	2565 ± 90	819 cal BC	888 BC
	89	2880 ± 50	846 cal BC	931 BC
	90	2790 ± 60	873 cal BC	974 BC
2	92	2775 ± 45	927 cal BC	996 BC
	94	2885 ± 45	981 cal BC	1080 BC
	96	2925 ± 45	1034 cal BC	1164 BC
1	98	2915 ± 60	1088 cal BC	1201 BC
	100	2900 ± 60	1142 cal BC	1248 BC
	102	3135 ± 60	1195 cal BC	1295 BC
	104	2875 ± 60	1249 cal BC	1342 BC
	110	3145 ± 45	1410 cal BC	1484 BC

the wiggle-match procedure and to model a "depth" scale based on the AP concentration.

We calculated the average arboreal pollen concentration ($\bar{A}$) from the smoothed concentration (A) for the interval 110-56 cm and the deviation of each sample from the average ($A/\bar{A}$). This last figure is a measure for the accumulation rate. The cumulative deviations were calculated and subsequently added to the depth of the upper sample to obtain the modelled "depth" scale (Table 5) based on a constant arboreal pollen accumulation rate. Each sample in the modelled scale has an AP concentration equivalent to the average concentration. The calculated distance between subsequent ^{14}C dates was used in the wiggle-match procedure. In Fig. 7 and Table 5 the results of the wiggle-match of the complete data set with modelled sample distance are shown. From 1432 cal BC to ca. 800 cal BC the match of the ^{14}C dates to the calibration curve is satisfactory, but from ca. 800 cal BC onwards the ^{14}C dates do not fit the calibration curve. This is because of the distribution of the samples at 86, 84, 83, 81, 79, and 77 cm depth which appear to be plotted too close to each other as a result of the modelled distance between ^{14}C samples. Due to the relatively low values of the arboreal pollen concentration between 86 and 77 cm depth, in the sample-distance modelling this interval was attributed a relatively large accumulation rate, which is not confirmed by the wiggle-matched result. It seems that in this interval the observed low pollen concentration values were determined partly by a high accumulation rate (in this interval about 80% of peat is composed of fast-growing *Sphagnum*; Fig. 5), but also by a relatively low arboreal pollen influx. Deforestation can be excluded as a cause of this decrease of arboreal pollen influx. Although scattered grains of Cerealia-type and *Secale* pollen were found throughout the whole analysed sequence (ca. 4100 BP to the present time), most likely coming from the lowlands of Silesia and Bohemia, no episode of deforestation was recorded

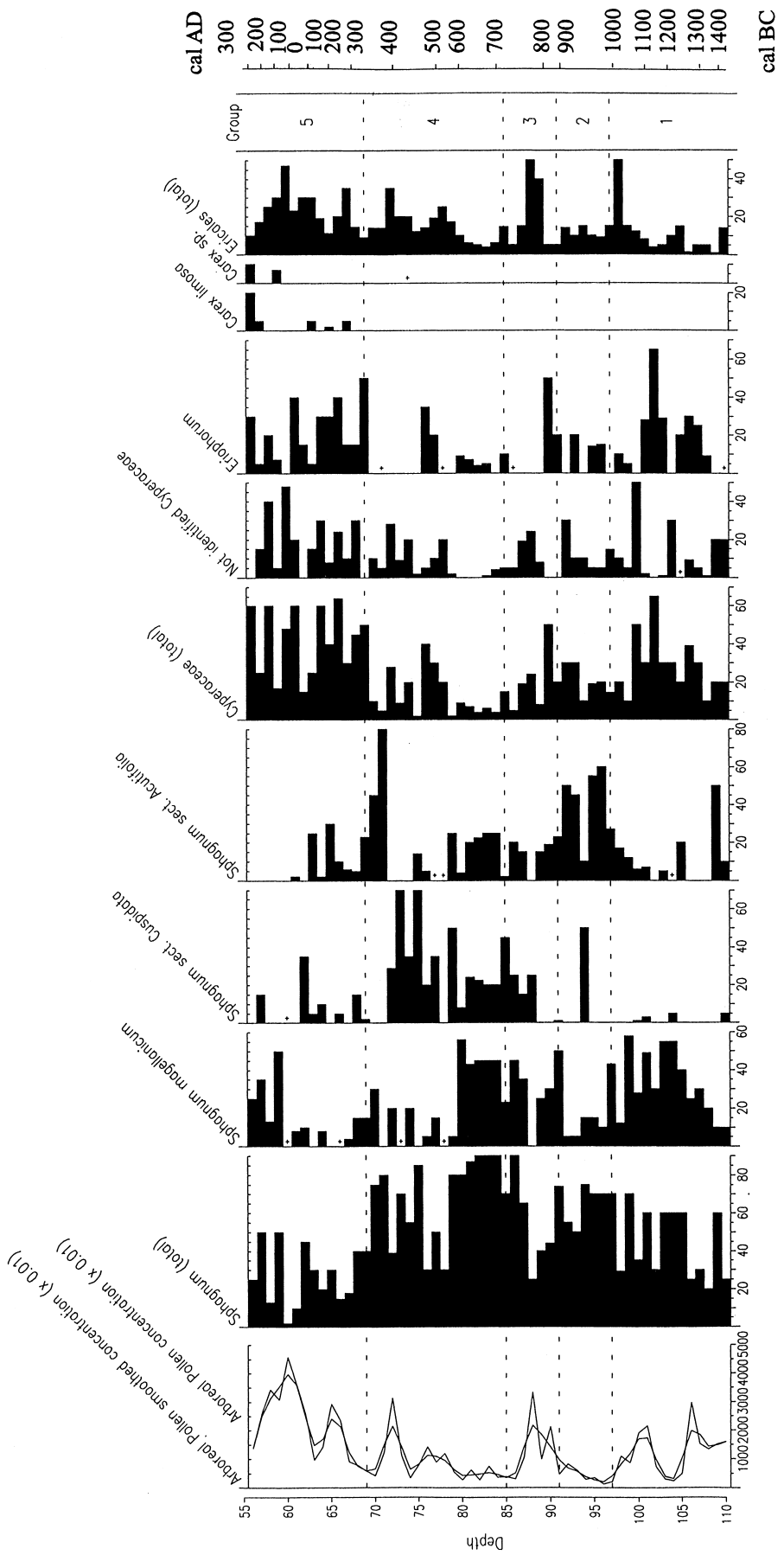

Fig. 5. Arboreal pollen concentrations as a function of depth, and selected macrofossil curves. The values of concentrations and smoothed concentrations are multiplied by 0.01 and are expressed in number of pollen grains per cc of peat. The *x*-axis scale for the macrofossil histograms is the estimated percentage in volume of each constituent within the total composition of the sample. The time-scale is based on the results of wiggle-match dating of sub-sets with "tree-pollen modelled" sample-distances. The dashed lines indicate the division in groups from 1 to 5, used for achieving a solution for the time-control; this solution was considered not optimal and was then rejected. The division in three groups used for the optimal time-control is shown in Fig. 7 and Table 5.

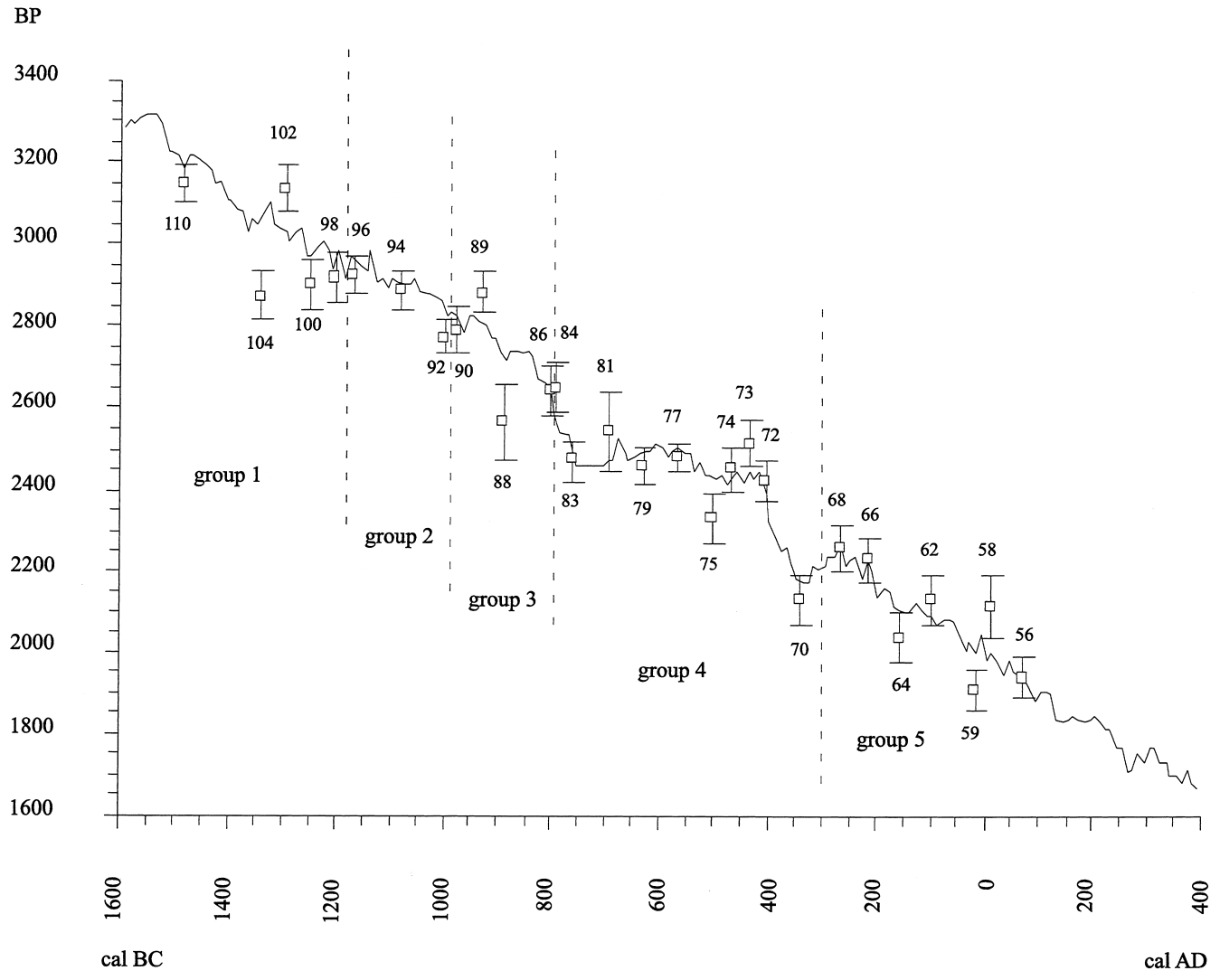

Fig. 6. Wiggle-match per sub-dataset: group 1 (110–98 cm); group 2 (96–92 cm); group 3 (90–86 cm); group 4 (84–70 cm); group 5 (68–56 cm). The resulting calendar ages are reported in Table 5. Each date is given with its standard deviation (error bar) and with its depth in the peat sequence (in cm).

until the 11th century AD (unpublished data). In the time-span considered in this paper, single grains of Cerealia-type and *Secale* occurred (Fig. 8; note that these curves are exaggerated by a factor 6) but no evidence of deforestation is observed on arboreal pollen percentages. The low influx might be the effect of changes in composition of the local peat forming vegetation, that influenced pollen collecting efficiency. Another hypothesis on the causes of the decrease in tree-pollen influx might be the onset of a climatic deterioration at approximately 850–760 cal BC (van Geel and Renssen, 1998). In fact, the decrease of arboreal pollen influx occurred in correspondence with the rapid increase of ^{14}C in the atmosphere due to a lower solar activity (Stuiver and Braziunas, 1993). The Pančavská Louka site is located at the forest limit in a mountainous area. In this situation, pollen production is dependent on the length of the growing season and on the occurrence of late frost, the latter a factor that can damage the flowers and hamper pollen production and dispersal. In case of a climatic change determining a late persistence of the snow cover, pollen grains that were deposited on the snow might have been drained away at the thaw. In both cases: lower pollen production or "pollen drainage", a lower arboreal pollen concentration can be expected. The composition of the peat shows additional evidence for the occurrence of climatic change at 88 cm depth where wet-growing *Sphagnum* sect. *Cuspidata* becomes one of the main elements (it is usually above 20% in volume) of the peat forming vegetation, and at 87 cm depth where the total volume attained by *Sphagnum* species grows to approximately 80% (Fig. 5). These events can be interpreted as

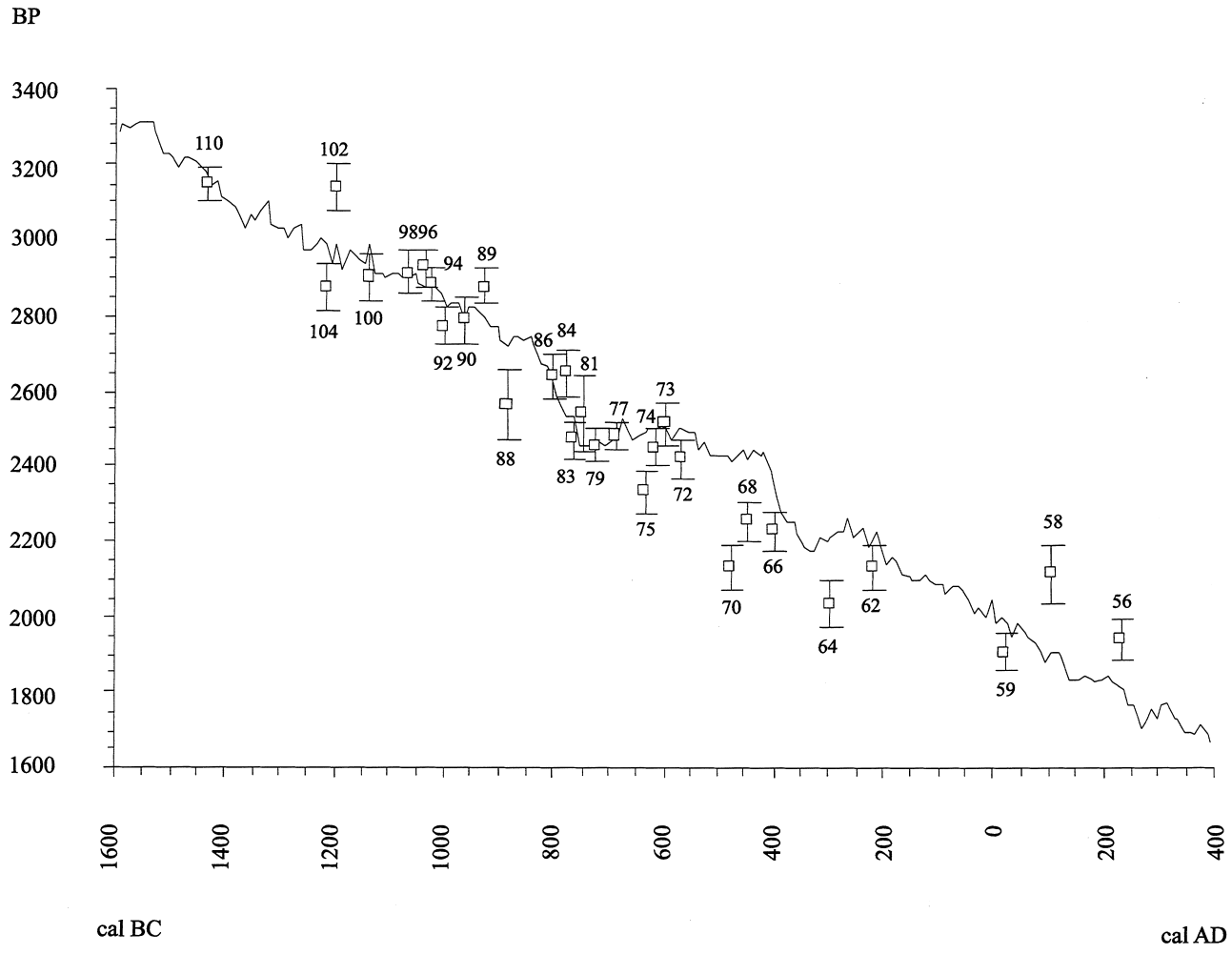

Fig. 7. Wiggle-match of the complete set of 29 dates from Pančavská Louka using modelled inter-sample distance based on tree pollen concentrations (for details see text). Each date is given with its standard deviation (error bar) and with its depth in the peat sequence (in cm).

the combined effect of higher precipitation (favouring *Sphagnum* growth, especially *Sphagnum* sect. *Cuspidata*) and cooler conditions (inhibiting decomposition and reducing evapotranspiration).

Due to a low pollen influx in the samples between 86 and 77 cm depth, we divided the dataset in three parts — from 110 to 88 cm, from 86 to 77 cm and from 75 to 56 cm — and independently matched each part to the calibration curve. The results of the wiggle-match of the three sub-datasets are shown in Fig. 9 and Table 5. We observed that the samples from 102 and 58 cm depth do not fit the calibration curve: they show older radiocarbon ages. During the selection procedures these samples were assigned a fungal infection coefficient of respectively 1–1.5 and 1; we conclude that a residual fungal contamination was probably still present in these samples after the cleaning procedures and thus fungal remains may have determined a reservoir effect (Kilian et al., 1995).

4. Discussion

The result of the calibration of each individual ^{14}C date presented in Table 2 yields the problem of interpreting the probability intervals. Each calendar age has to fall inside the limits indicated by the probability distribution, i.e. between the oldest and the youngest possible calendar age. If we choose the 2σ probability distribution for each calibration (95.4% confidence level), the oldest and the youngest limits (Fig. 10) define a possible range of approximately 250–300 yr. The radiocarbon dates corresponding to the plateau in the calibration curve have even wider ranges (350–400 yr). The single calendar ages chosen as arithmetic average or "best fit" display an uncertainty of approximately 125–150 yr (half the range). For the sample at 90 cm depth (2790 ± 60 BP), for instance, whose calibration range is 1125 to 824 cal BC, the uncertainty for the arithmetic mean of the

Table 5
Modelled inter-sample distance and calendar ages resulting from respectively the wiggle-match of the complete data-set and of the sub-datasets with a modelled inter-sample distance. The sub-datasets are: group 1 (110 to 88 cm); group 2 (86 to 77 cm); group 3 (75 to 56 cm). The inter-sample distance is modelled on changes in arboreal pollen concentrations. The division in the sub-datasets is necessary to fit also the samples from 86 to 77 cm depth to the calibration curve

Sub-datasets	Depth (cm)	Modelled sample distance (cm)	WMD modelled distance Complete dataset	WMD modelled distance Sub-datasets
3	56.0	56.0537173	234 cal AD	324 cal AD
	58.0	60.3401709	103 cal AD	200 cal AD
	59.0	63.0361751	20 cal AD	123 cal AD
	62.0	70.6661938	216 cal BC	96 cal BC
	64.0	73.0898818	298 cal BC	166 cal BC
	66.0	76.539458	400 cal BC	265 cal BC
	68.0	78.0577217	449 cal BC	309 cal BC
	70.0	79.0059193	478 cal BC	336 cal BC
	72.0	81.7831332	564 cal BC	416 cal BC
	73.0	82.8675907	598 cal BC	447 cal BC
	74.0	83.3569118	613 cal BC	461 cal BC
	75.0	83.9936415	633 cal BC	480 cal BC
2	77.0	85.6965751	686 cal BC	584 cal BC
	79.0	86.9194101	724 cal BC	657 cal BC
	81.0	87.5855463	745 cal BC	697 cal BC
	83.0	88.3525437	768 cal BC	743 cal BC
	84.0	88.7060289	779 cal BC	765 cal BC
	86.0	89.366353	800 cal BC	799 cal BC
1	88.0	92.124935	885 cal BC	828 cal BC
	89.0	93.5431447	929 cal BC	879 cal BC
	90.0	94.6323872	963 cal BC	917 cal BC
	92.0	95.8969885	1002 cal BC	963 cal BC
	94.0	96.6274752	1025 cal BC	989 cal BC
	96.0	96.9931551	1036 cal BC	1001 cal BC
	98.0	97.938983	1066 cal BC	1035 cal BC
	100.0	100.158497	1135 cal BC	1114 cal BC
	102.0	102.246061	1200 cal BC	1189 cal BC
	104.0	102.793734	1216 cal BC	1208 cal BC
	110.0	110	1432 cal BC	1456 cal BC

calibration range (974 cal BC) is $\pm$ 150.5 years and that of the "best fit" (963 cal BC) is $+162/-139$ yr. The researcher pursuing a detailed reconstruction of vegetation development, climatic change or human activities, or, even more critical, applying spectral analysis techniques on sequences of palaeoecological data, needs to attribute a singular age to each sample. Reducing the results of the calibration to a single age represents an arbitrary solution that inevitably leads to relatively large errors and thus is not a valid method to translate radiocarbon dates into calendar ages in correspondence with wiggles in the calibration curve.

The application of the wiggle-match strategy to the complete data set is shown in Fig. 4 and the results are presented in Table 4. The results of the wiggle-matching of the complete data set represent an improvement if compared with those of the calibration of each ^{14}C date because the changes in ^{14}C concentration in the atmosphere are used to attain a higher degree of precision. In this respect, WMD shows an opposite behaviour compared with calibration of a single date: in the presence of wiggles, WMD increases the accuracy of the result while calibration of separate dates provides relatively wide probability ranges in calendar time.

The wiggle-matching of each separate sub-dataset (Fig. 6), divided according to the main changes in arboreal pollen concentration (Fig. 5), are a further improvement as the main changes in peat accumulation rate are — at least qualitatively — considered.

A sample distance modelled on changes in arboreal pollen concentration shows improved wiggle-matching results. Here the arboreal pollen concentration quantitatively establishes the inter-sample distance between the ^{14}C dates used for the wiggle-match. In the wiggle-match of the data set with modelled sample distances (Fig. 7) the position of the ^{14}C dates validates the modelled scale,

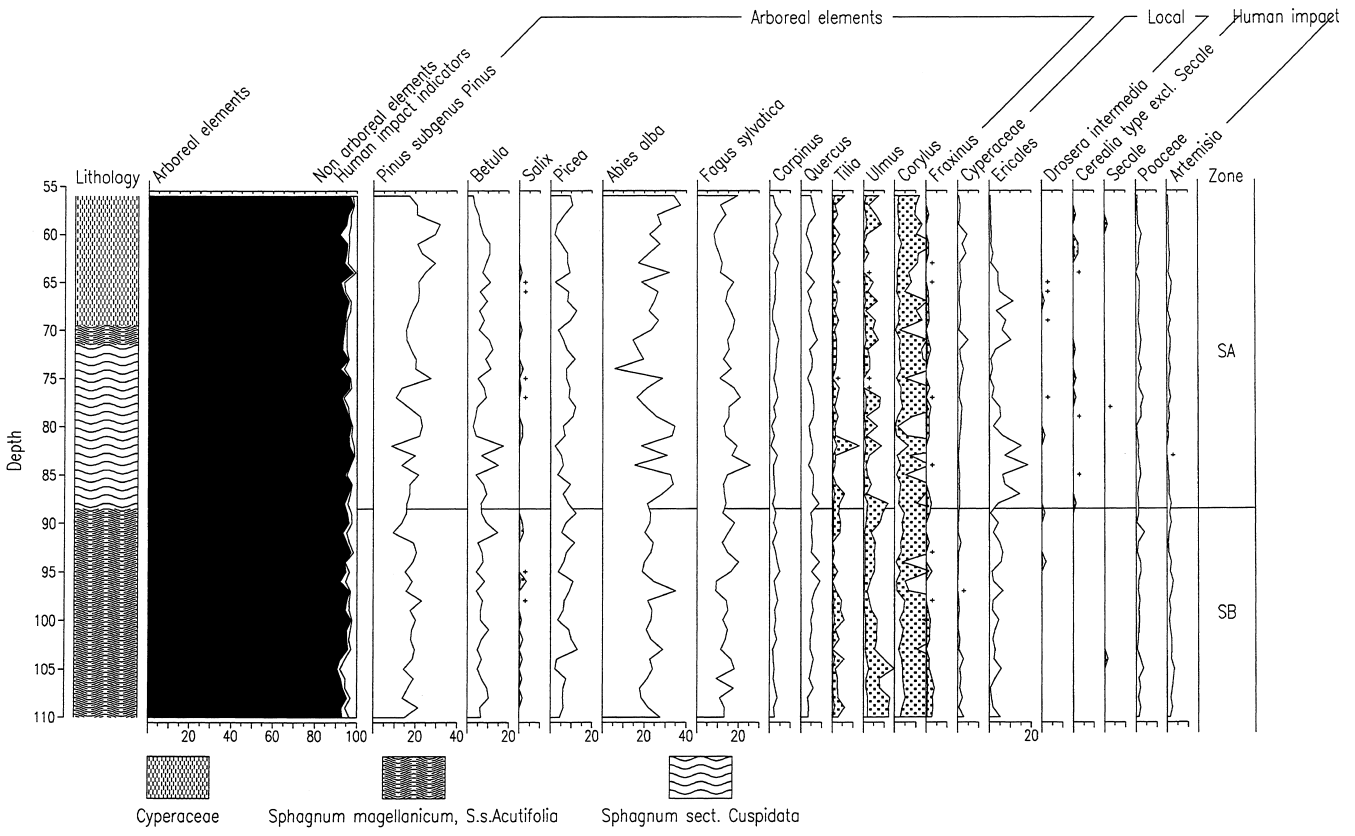

Fig. 8. Selection of pollen curves. The lithology shows dominant taxa only. For more information about peat forming taxa see Fig. 5. Local elements are not in the pollen sum. The curves with dotted pattern were exaggerated by a factor 6. SB = Subboreal, SA = Subatlantic

except for the groups of dates from 86 to 77 cm, probably indicating that in this interval a low pollen influx (and not only an increased peat accumulation rate) partly determined the observed low arboreal pollen concentrations. The division of the data set in three subsets (110 to 88 cm, 86 to 77 cm and 75 to 56 cm) and the independent match of the three sets, definitely solves the problem of the differences in accumulation rate and in pollen influx. We consider these results (Fig. 9; Table 5) as the optimal solution for time-control achievement over the sequence of Pančavská Louka. In Fig. 10 we compare the results of the calibration and of WMD. For the calibration, both the use of the average of the 2σ probability distribution and the "best fit" to the calibration curve results in an irregularly fluctuating time–depth relation, hardly to be expected in a natural situation. The results of the different attempts of WMD show similar time–depth relations, linear or quasi-linear. The results of the wiggle-match of the complete dataset with modelled (on the arboreal pollen concentrations) sample distance show a discrepancy in the interval between approximately 800 and 100 cal BC; this discrepancy is probably due to the fact that the fluctuating pollen influx between 800 and 600 cal BC compromised the wiggle-match of the younger levels. The linearity of the results of the WMD of the sets with conventional depth scale derives from the distribution of the dates in the program Cal25 that is linear by default for each data-set. The time–depth relation provided by the WMD of the sub-data-sets with modelled sample distance (Fig. 11) shows a sinusoidal trend in the accumulation rates, with quasi-linear accumulation rates inside intervals with homogeneous peat composition, and smooth, flowing changes in accumulation rate at the transition between intervals with different peat composition. A correspondence is observed between the peat composition and the accumulation rate: high *Sphagnum* volume percentages correspond to high peat accumulation rates, whereas high Cyperaceae percentages seem to have caused low accumulation rates. The higher rates of peat accumulation occur in the intervals from 97 to 91 cm depth and from 87 to 68 cm depth where the percentage of *Sphagnum* is generally higher than 65% and that of Cyperaceae lower than 25%; the interval from 87 to 68 cm depth corresponds with the nearly continuous presence of wet-growing *Sphagnum* sect. *Cuspidata* (Fig. 5). The lowest peat accumulation rates are attained from 110 to 97 cm depth, and from 68 to 56 cm depth, where *Sphagnum* attains usually between 20 and

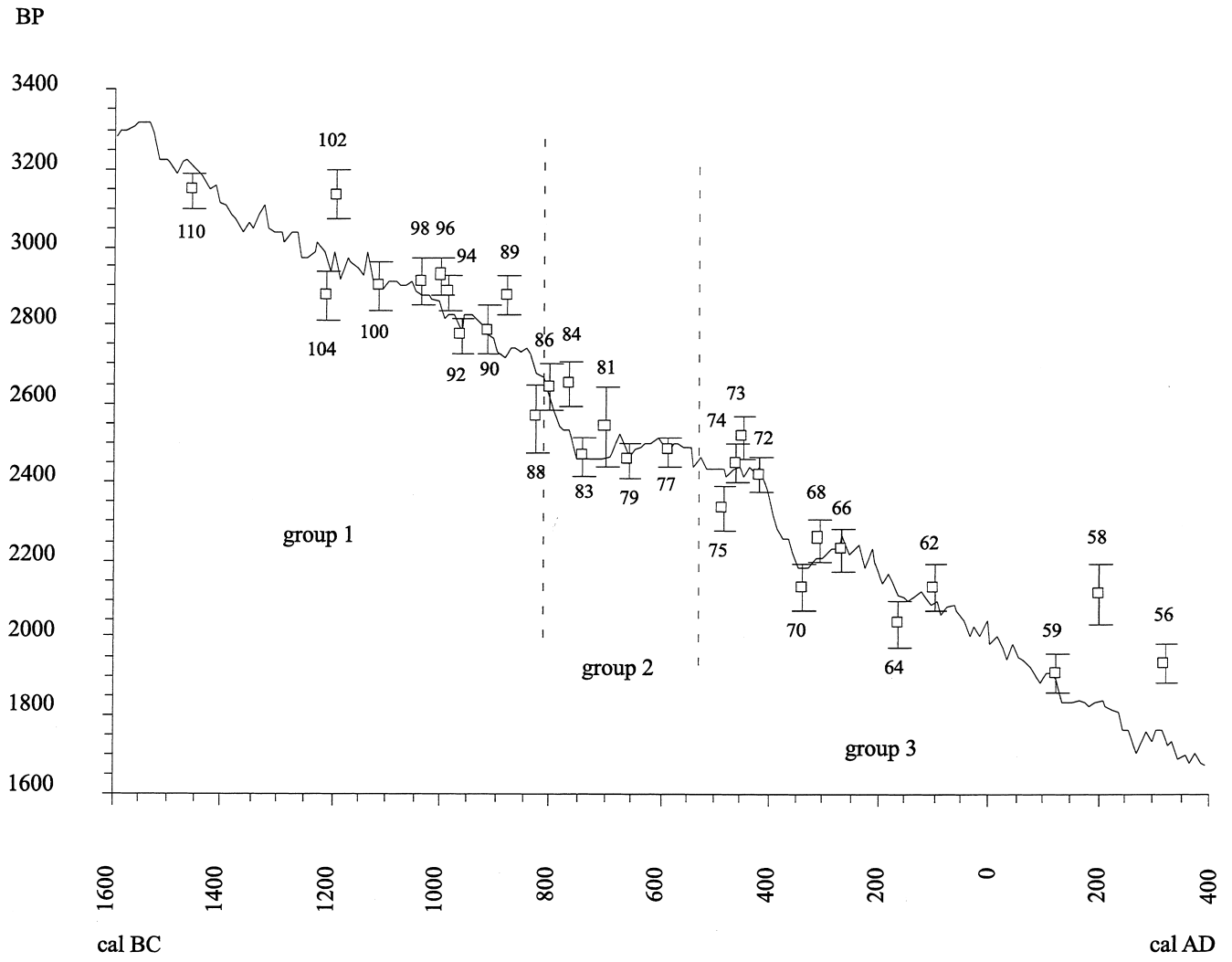

Fig. 9. Wiggle-match of the sub-datasets from Pančavská Louka with inter-sample distance modelled on tree-pollen concentrations: group 1 (110–88 cm); group 2 (86–77 cm); group 3 (75–56 cm). Each date is given with its standard deviation (error bar) and with its depth in the peat sequence (in cm).

40% of the volume of the peat and Cyperaceae percentages are usually 30% or more.

This time–depth relation well describes a natural peat accumulation in time; it avoids both linearity—hardly compatible with natural phenomena—and sharp steps at the border of two adjacent sub-datasets; this last feature may result from the separate wiggle-matching of data, and it is justifiable only if hiatuses or discontinuities in the peat sequence go together with steps in the time–depth relation.

5. Conclusions

To achieve an optimal time control for the late Subboreal—early Subatlantic time interval of the Pančavská Louka peat sequence, both the calibration of separate ^{14}C dates and the wiggle-match strategy were applied. As the considered interval included the period around 850–760 BC, characterised by a decrease in solar activity and a sharp increase of $\Delta^{14}C$ (van Geel et al., 1998), the chosen method for transforming the radiocarbon time-scale into calendar time-scale needs to take into account these large atmospheric ^{14}C variations. The calibration of most dates yields inaccurate results (wide, and often not continuous calendar age ranges) in this interval. The wiggle-match strategy yields better results because it uses the known atmospheric ^{14}C changes in combination with the stratigraphical order of the dates. The best results of wiggle-match dating were obtained using changes in the peat accumulation rate, as apparent from the arboreal pollen concentrations, and taking into account a lower pollen influx in a number of samples between approximately 800 and 600 cal BC. The WMD results are precise enough to allow time-control for complex palaeoecological analyses such as spectral analysis. Our strategy

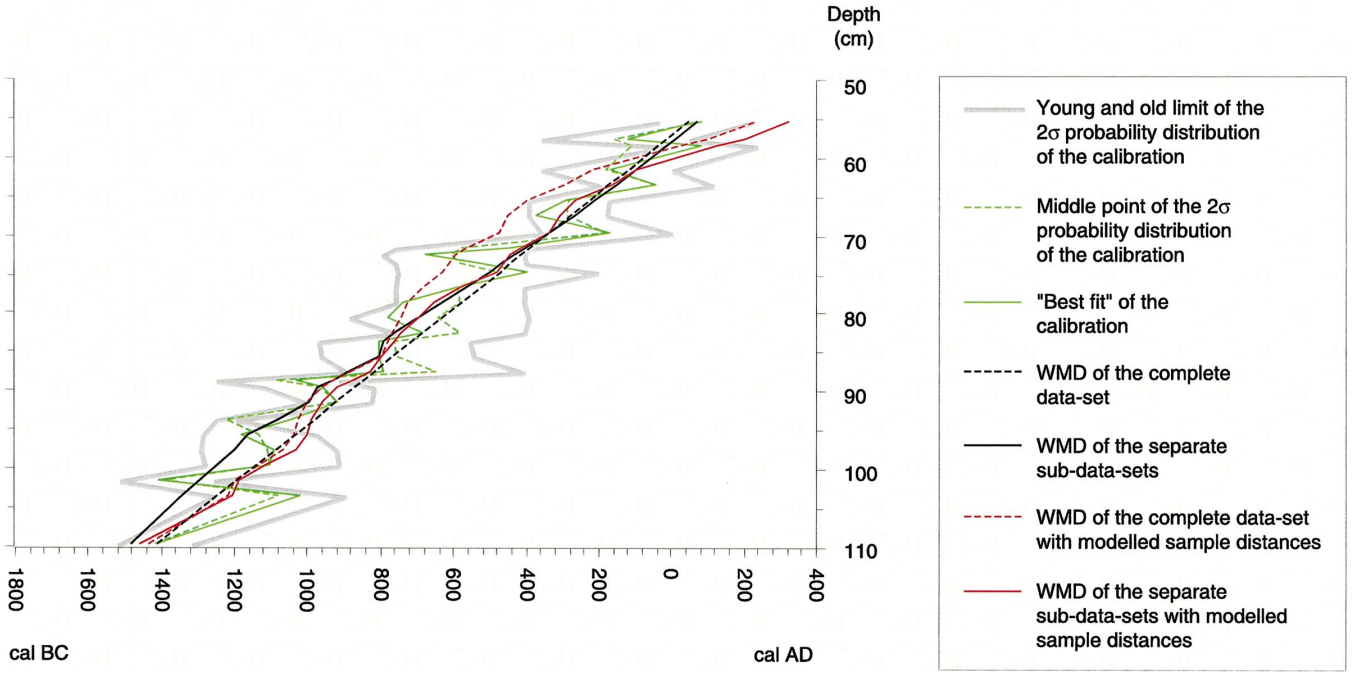

Fig. 10. Time–depth relations obtained from the calibration of the ^{14}C dates (oldest and youngest interval limits of the 2σ probability distribution, middle point of the calibration and "best fit") and from the wiggle-matching dating of the complete dataset, of sub-datasets and wiggle-matching dating of the complete dataset with modelled sample distance and of the sub-data-sets with modelled sample distance.

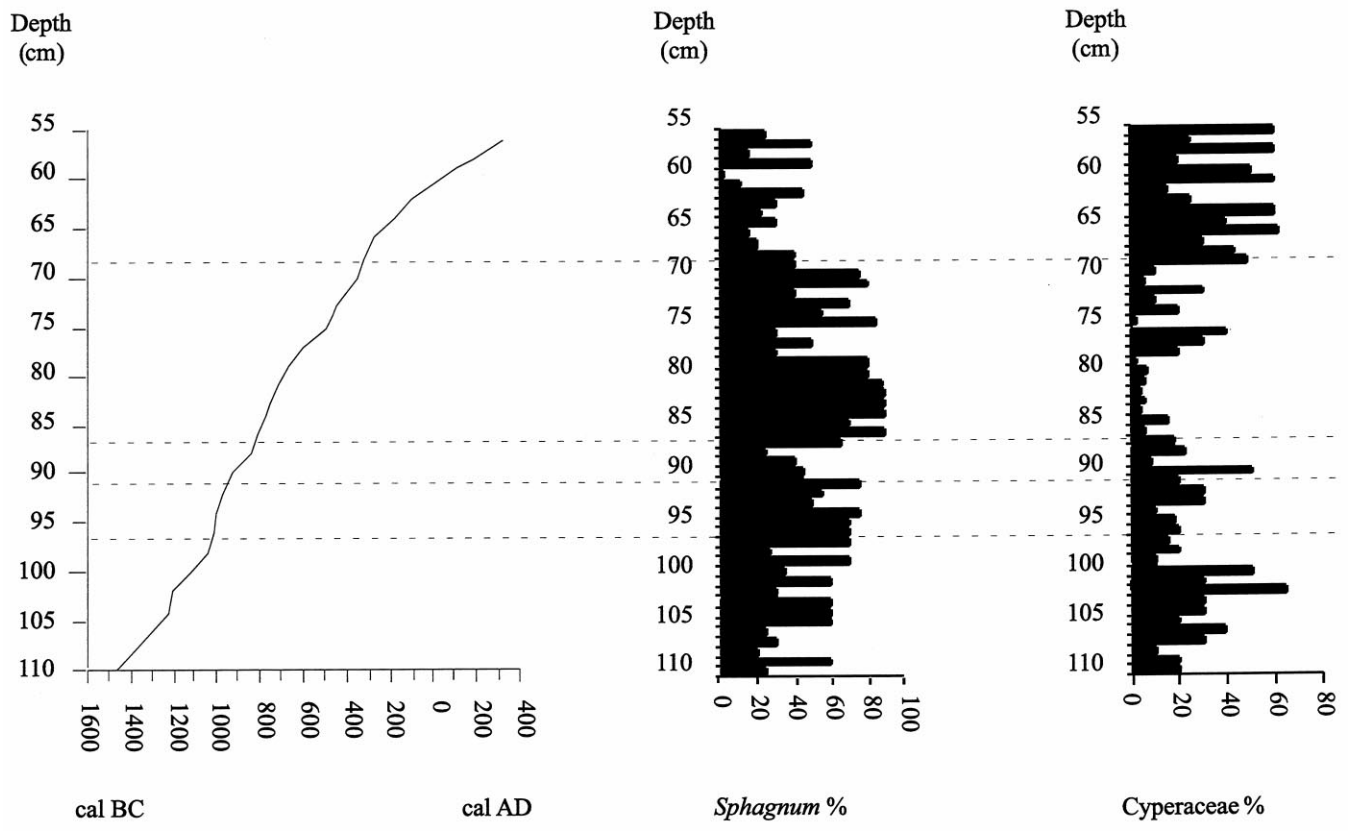

Fig. 11. Time-depth relation based on the results of wiggle-match dating of sub-datasets with a modelled sample distance. The peat accumulation rate follows a sinusoidal curve with lower accumulation rates when macrofossils of Cyperaceae show a high representation, and higher accumulation rates when *Sphagna* were dominant peat formers (> 60%).

represents the best solution achievable today for the conversion from the radiocarbon to the calendar timescale in peat deposits. Accurate selection and handling of the samples are a prerequisite for obtaining reliable results. Finally, we conclude that the local vegetation succession, in relation to the changes in atmospheric radiocarbon content, shows additional evidence for solar forcing of climate change at the Subboreal – Subatlantic transition.

Acknowledgements

We are grateful to the staff of the Krkonoše National Park (Czech Republic), particularly Dr. Jiří Flousek, Head of the Department of Nature Protection, for the permission to sample in the territory of the Park. We would like to thank Mrs. Anita Aerts-Bijma, Mrs. Dicky van Zonneveld and Mr. Fsaha Ghebru of the Centre for Isotope Research of the University of Groningen for the help and the support during the preparation of the radiocarbon samples, and Mrs. Annemarie Philip of the Hugo de Vries Laboratory of the University of Amsterdam for the preparation of the pollen samples. Dr. Igino Emmer is thanked for his help during the fieldwork and Dr. Herman Mommersteeg for the discussion and his help during the fieldwork, and Dr. Dmitri Mauquoy for having improved the English in the manuscript. We are grateful to Dr. Keith Barber and Dr. Michel Magny for their remarks on the manuscript.

References

Aerts-Bijma, A.T., Meijer, H.A.J., van der Plicht, J., 1997. AMS sample handling in Groningen. Nuclear Instruments and Methods B 123, 221–225.

Bennett, K.D., 1995. Confidence intervals for age estimates and deposition times in late-Quaternary sediment sequences. The Holocene 4, 337–348.

Clymo, R.S., 1963. Ion exchange in *Sphagnum* and its relation to bog ecology. Annals of Botany 27, 309–324.

Davis, O.K., 1994. The correlation of summer precipitation in the southwestern U.S.A. with isotopic records of solar activity during the medieval warm period. Climatic Change 26, 271–287.

Denton, G.H., Karlen, W., 1973. Holocene climatic variation — their pattern and possible cause. Quaternary Research 3, 155–205.

de Vries, H., 1958. Variations in concentration of radiocarbon with time and location on Earth. Koninklijke Nederlandse Akademie van Wetenschappen, Proceedings Serie Vol. B 61, pp. 1–9.

Dumayne, L., Stoneman, R., Barber, K., Harkness, K., 1995. Problems associated with correlating calibrated radiocarbon-dated diagrams with historical events. The Holocene 5 (1), 118–123.

Faegri, K., Iversen, J., 1989. Textbook of Pollen Analysis. Wiley, Chichester.

Jirikowic, J.L., Kalin, R.M., Davis, O.K., 1993. Tree-ring ^{14}C as an indicator of climatic change. Proceedings, Chapman Conference. Jackson Hole, Wyoming, AGU, Geophysical Monographies 78, 353–366.

Karlen, W., Kuylenstierna, J., 1996. On solar forcing of the Holocene climate: evidence from Scandinavia. The Holocene 6 (3), 359–365.

Kilian, M.R., van Geel, B., van der Plicht, J., 2000. ^{14}C AMS wiggle-matching of raised bog deposits and models of peat accumulation. Quaternary Geochronology (in press).

Kilian, M.R., van der Plicht, J., van Geel, B., 1995. Dating raised bogs: new aspects of AMS ^{14}C wiggle matching, a reservoir effect and climatic change. Quaternary Science Reviews 14, 959–966.

Magny, M., 1993. Solar influences on Holocene climatic changes illustrated by correlations between past lake-level fluctuations and the atmospheric ^{14}C record. Quaternary Research 40, 1–9.

Magny, M., 1999. Lake-level fluctuations in the Jura and French subalpine ranges associated with ice-rafting events in the North Atlantic and variations in the polar atmospheric circulation. Geographie Physique et Quaternaire 10, 61–64.

Middeldorp, A.A., 1982. Pollen concentration as basis for indirect dating and quantifying net organic and fungal production in a peat bog ecosystem. Review of Palaeobotany and Palynology 37, 225–282.

Mook, W.G., Streurman, H.J., 1983. Physical and chemical aspects of radiocarbon dating. Pact 8 (Proceedings of the 1st International Symposium ^{14}C and Archaeology, Groningen 1981), 31–55.

Moore, P.D., Webb, J.A., Collinson, M.E., 1991. Pollen Analysis. Blackwell Scientific Publications, Oxford.

Mous, D.J.W., Gottdang, A., van der Plicht, J., Wijma, S., Zondervan, A., 1995. Progress at the Groningen AMS facility. Nuclear Instruments and Methods in Physics Research B 99, 532–536.

Neuhäuslova, Z., Blažková, D., Grulich, V., Husová, M., Chytrý, M., Jeník, J., Jirásek, J., Kolbek, J., Kropáč, Z., Ložek, V., Moravec, J., Prach, K., Rybníček, K., Rybníčková, E., Sádlo, J., 1998. Map of Potential Natural Vegetation of the Czech Republic. Academia: Praha.

Pearson, G.W., 1986. Precise calendrical dating of known growth-period samples using a "curve fitting" technique. Radiocarbon 28, 292–299.

Stuiver, M., Braziunas, T.F., 1993. Sun, ocean, climate and atmospheric $^{14}CO_2$: an evaluation of causal and spectral relationships. The Holocene 3, 289–305.

Stuiver, M., Reimer, P.J., Bard, E., Beck, J.W., Burr, G.S., Hughen, K.A., Kromer, B., McCormac, F.G., van der Plicht, J., Spurk, M., 1998. INTCAL98 Radiocarbon Age Calibration, 24,000 - 0 cal BP. Radiocarbon 40 (3), 1041–1083.

Suess, H.E., 1970. The three causes of secular ^{14}C fluctuations, their amplitudes and time constants. In: Olsson, I.U. (Ed.), Radiocarbon Variations and Absolute Chronology. Proceedings of the 12th Nobel Symposium. Almqvist and Viksell, Stockholm, pp. 595–605.

van der Plicht, J., 1993. The Groningen radiocarbon calibration program. Radiocarbon 35, 231–237.

van der Plicht, J., Mook, W.G., 1987. Automatic radiocarbon calibration: illustrative examples. Palaeohistoria 29, 173–182.

van Geel, B., van der Plicht, J., Kilian, M.R., Klaver, E.R., Kouwenberg, J.H.M., Renssen, H., Reynaud-Farrera, I., Waterbolk, H.T., 1998. The sharp rise of $\Delta^{14}C$ ca. 800 cal BC: possible causes, related climatic teleconnections and the impact on human environments. In: Mook, W.G., and van der Plicht, J. (Eds.), Proceedings of the 16th International ^{14}C Conference, Radiocarbon 40, 535–550.

van Geel, B., Mook, W.G., 1989. High resolution ^{14}C dating of organic deposits using natural atmospheric ^{14}C variations. Radiocarbon 31, 151–155.

van Geel, B., Raspopov, O.M., Renssen, H., van der Plicht, J., Dergachev, V.A., Meijer, H.A.J., 1999. The role of solar forcing upon climate change. Quaternary Science Reviews 18, 331–338.

van Geel, B., Renssen, H., 1998. Abrupt climate change around 2650 BP in NW-Europe: evidence for climatic teleconnections and a tentative explanation. In: Issar, A.S., Brown, N. (Eds.), Water, Environment and Society in Times of Climatic Change. Kluwer, Dordrecht, pp. 21–41.

Vogel, J.C., Southon, J.R., Nelson, D.E., Brown, T.A., 1984. Performance of catalytically condensed carbon for use in accelerator mass spectrometry. Nuclear Instrument and Methods 233 (B5), 289–293.